2003-12-20

Search For High-Energy Gamma Rays From An X-Ray-Selected Blazar Sample

P. T. Reynolds
Cork Institute of Technology

Et. al.

Recommended Citation

De la Calle Perez, I. et al., 2003. Search for High-Energy Gamma Rays from an X-Ray–selected Blazar Sample. The Astrophysical Journal, 599(2), pp.909–917. Available at: http://dx.doi.org/10.1086/379544.

The Astrophysical Journal, 599:909–917, 2003 December 20

SEARCH FOR HIGH-ENERGY GAMMA RAYS FROM AN X-RAY–SELECTED BLAZAR SAMPLE

I. de la Calle Pérez,[1] I. H. Bond,[1] P. J. Boyle,[2] S. M. Bradbury,[1] J. H. Buckley,[3] D. A. Carter-Lewis,[4] O. Celik,[5] W. Cui,[6] C. Dowdall,[7] C. Duke,[8] A. Falcone,[6] D. J. Fegan,[9] S. J. Fegan,[10,11] J. P. Finley,[6] L. Fortson,[2] J. A. Gaidos,[6] K. Gibbs,[10] S. Gammell,[9] J. Hall,[12] T. A. Hall,[13] A. M. Hillas,[1] J. Holder,[1] D. Horan,[10] M. Jordan,[3] M. Kertzman,[14] D. Kieda,[12] J. Kildea,[9] J. Knapp,[1] K. Kosack,[3] H. Krawczynski,[3] F. Krennrich,[4] S. LeBohec,[4] E. T. Linton,[2] J. Lloyd-Evans,[1] P. Moriarty,[7] D. Müller,[2] T. N. Nagai,[12] R. A. Ong,[5] M. Page,[8] R. Pallassini,[1] D. Petry,[4,15] B. Power-Mooney,[9] J. Quinn,[9] P. Rebillot,[3] P. T. Reynolds,[16] H. J. Rose,[1] M. Schroedter,[10,11] G. H. Sembroski,[6] S. P. Swordy,[2] V. V. Vassiliev,[12] S. P. Wakely,[2] G. Walker,[12] and T. C. Weekes[10]

Received 2003 July 1; accepted 2003 September 3

ABSTRACT

Our understanding of blazars has been greatly increased in recent years by extensive multiwavelength observations, particularly in the radio, X-ray, and gamma-ray regions. Over the past decade the Whipple 10 m telescope has contributed to this with the detection of five BL Lacertae objects at very high gamma-ray energies. The combination of multiwavelength data has shown that blazars follow a well-defined sequence in terms of their broadband spectral properties. Together with providing constraints on emission models, this information has yielded a means by which potential sources of TeV emission may be identified and predictions made as to their possible gamma-ray flux. We have used the Whipple telescope to search for TeV gamma-ray emission from eight objects selected from a list of such candidates. No evidence has been found for very high energy emission from the objects in our sample, and upper limits have been derived for the mean gamma-ray flux above 390 GeV. These flux upper limits are compared with the model predictions, and the implications of our results for future observations are discussed.

Subject headings: BL Lacertae objects: individual (RGB J0214+517, RGB J1117+202, RGB J1725+118, 1ES 0033+595, 1ES 0120+340, 1ES 0229+200, 1ES 0806+524, 1ES 1426+428, 1ES 1553+113, 1ES 1959+650) — gamma rays: observations

1. INTRODUCTION

According to the unified scheme of active galactic nuclei (AGNs), a blazar is considered to be any radio-loud AGN that displays highly variable, beamed, nonthermal emission from radio to gamma-ray wavelengths (Urry & Padovani 1995). The nonthermal emission is believed to originate from a population of electrons moving with relativistic velocity along a plasma jet oriented at a small angle to the line of sight (e.g., Sikora 1994). In a $\nu F(\nu)$ plot, the spectral energy distribution (SED) of blazars shows two broad peaks, one at energies ranging from the infrared to the X-ray band and the other in the gamma-ray band. Two types of approaches have been taken to characterize the blazar SED: a phenomenological approach (Fossati et al. 1998), in which the bolometric source luminosity largely governs the blazar SED, and more model-dependent approaches. Several models have been put forward in an attempt to explain the blazar SED, the most frequently cited of which is the synchrotron self-Compton (SSC) model. In this model, the origin of the first peak is synchrotron emission from relativistic electrons, which are then upscattered by the inverse Compton (IC) process to form the second peak in the gamma-ray band (e.g., Bloom & Marscher 1996). In external Compton (EC) models, the synchrotron emission may be accompanied by ambient soft photons of different origin as a target for the IC process (Dermer & Schlickeiser 1993; Sikora, Begelman, & Rees 1994; Ghisellini & Madau 1996).

BL Lacertae (BL Lac) objects are a blazar subclass, characterized by their lack of strong emission or absorption lines, in which the second peak of the SED can extend up to very high (GeV–TeV) energies. They are therefore preferred targets of ground-based observations with atmospheric Cerenkov telescopes. Using these observations to determine the position of the second peak of the SED allows us to constrain associated parameters of emission models, most importantly, the intensity of the magnetic field and the maximum energy to which the particles responsible for the emission are accelerated (e.g., Buckley 1999).

TeV gamma rays from extragalactic sources suffer absorption by interaction with photons from the infrared

[1] Department of Physics, University of Leeds, Leeds LS2 9JT, Yorkshire, England, UK.
[2] Enrico Fermi Institute, University of Chicago, Chicago, IL 60637.
[3] Department of Physics, Washington University, St. Louis, MO 63130.
[4] Department of Physics and Astronomy, Iowa State University, Ames, IA 50011.
[5] Department of Physics, University of California, Los Angeles, CA 90095.
[6] Department of Physics, Purdue University, West Lafayette, IN 47907.
[7] School of Science, Galway-Mayo Institute of Technology, Galway, Ireland.
[8] Physics Department, Grinnell College, Grinnell, IA 50112.
[9] Physics Department, National University of Ireland, Belfield, Dublin 4, Ireland.
[10] Fred Lawrence Whipple Observatory, Harvard-Smithsonian Center for Astrophysics, Amado, AZ 85645.
[11] Department of Physics, University of Arizona, Tucson, AZ 85721.
[12] High Energy Astrophysics Institute, University of Utah, Salt Lake City, UT 84112.
[13] Department of Physics and Astronomy, University of Arkansas at Little Rock, Little Rock, AR 72204.
[14] Physics Department, De Pauw University, Greencastle, IN 46135.
[15] NASA Goddard Space Flight Center, Code 661, Greenbelt, MD 20771.
[16] Department of Physics, Cork Institute of Technology, Cork, Ireland.

(IR) background radiation (Gould & Schréder 1966; Primack et al. 1999; de Jager & Stecker 2002). A large TeV BL Lac object sample containing objects at a range of redshifts would provide the means to distinguish between intrinsic spectral features and the effects of absorption by the IR background. However, at present, the list of known TeV BL Lac objects is very small and needs to be expanded. The limited field of view of Cerenkov telescopes and their low duty cycle force us to select, a priori, the most promising target objects from a catalog of candidates for study. In the past, the Whipple collaboration has targeted the nearest northern hemisphere BL Lac objects, and this approach resulted in several positive detections: Mrk 421 ($z = 0.030$; Punch et al. 1992), Mrk 501 ($z = 0.034$; Quinn et al. 1996), and 1ES 2344+514 ($z = 0.044$; Catanese et al. 1998). In addition, observations of BL Lac objects with the peak of the first component of their SED extending far into the X-ray band (>0.1 keV) led to the detection of the most distant TeV source, 1ES 1426+428 ($z = 0.129$; Horan et al. 2002). Most recently, 1ES 1959+650 (Holder et al. 2003) was detected at TeV energies in an intense flaring state using the Whipple telescope. This object is also a close BL Lac object ($z = 0.048$), whose status as a TeV source was confirmed following marginal detection in 1998 at TeV energies by the Utah Seven-Telescope Array collaboration (Nishiyama et al. 1999).

In this paper, we report on candidate TeV sources selected following the work of Costamante & Ghisellini (2002). Their BL Lac object catalog is the first to provide estimates of TeV fluxes based on detailed model predictions and includes successful predictions of the TeV flux of 1ES 1959+650 in its flaring state (Aharonian et al. 2003). The catalog consists of objects bright in *both* the X-ray and radio bands, i.e., objects with *both* electrons energetic enough to upscatter seed photons to TeV energies *and* a high density of seed photons to be upscattered. The radio and X-ray fluxes are plotted in Figure 1, and as can be seen, the sample includes established TeV sources (including PKS 2155−304 [$z = 0.116$]; Chadwick et al. 1999). The gamma-ray flux at TeV energies is estimated by applying a homogeneous, one-zone SSC model (Ghisellini, Celotti, & Costamante 2002) and using the phenomenological parameterization of the blazar SED developed by Fossati et al. (1998) and adapted by Costamante & Ghisellini (2002). The latter approach by Costamante & Ghisellini (2002) was motivated by a desire to better describe the SEDs of low-power blazars. These flux estimates allow us to assess the detectability of this sample of BL Lac objects using present, or future, more sensitive, atmospheric Cerenkov telescopes. However, the dramatic variability of these sources significantly adds to the uncertainty of detecting a source at any given time.

We observed eight objects selected from this sample (§ 2). In §§ 3 and 4, we present a summary of the TeV data and discuss a new analysis method of background estimation suited to our observation strategy. The upper limits derived from our observations are summarized in § 5.1 and discussed within the framework of the popular emission models. Our observations are compared with the *Rossi X-Ray Timing Explorer* (*RXTE*) All-Sky Monitor (ASM) X-ray data where available (§ 5.2). In § 6. we discuss implications of nondetections of these candidates for future observations.

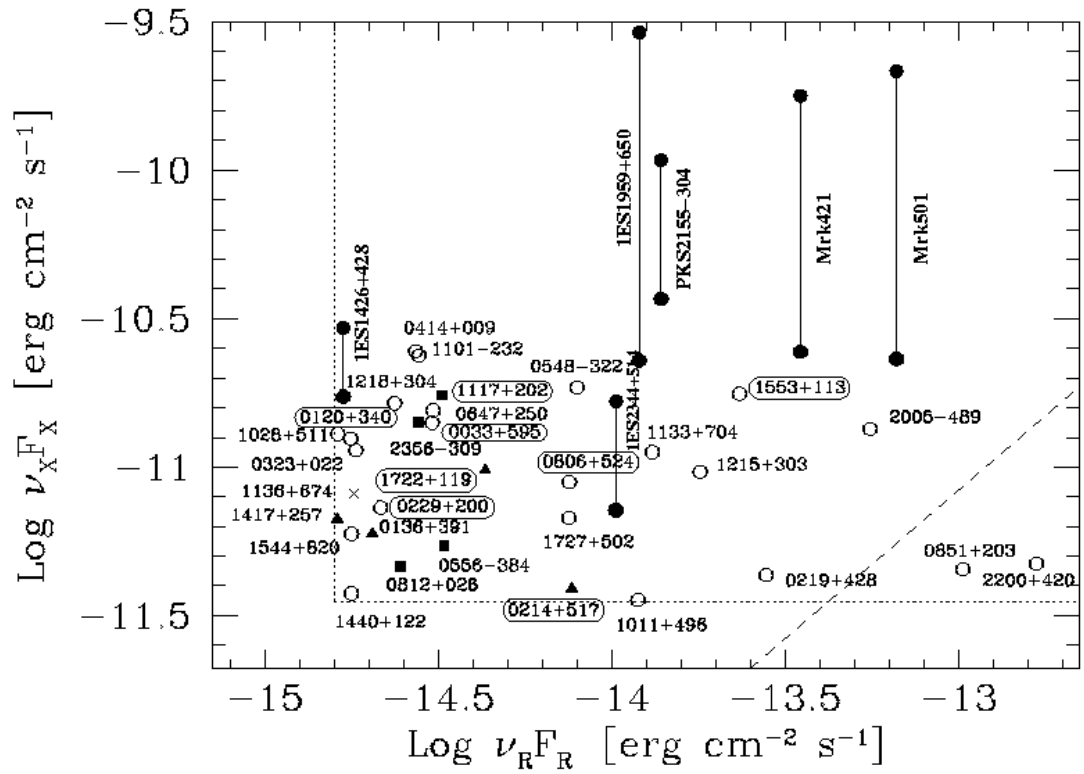

FIG. 1.—BL Lac objects in a $\nu F(\nu)$ plane. F_R and F_X represent the radio and X-ray flux at $\nu_R = 5$ GHz and $\nu_X = 1$ keV, respectively. Different symbols indicate different samples (see Costamante & Ghisellini 2002 for details). Encircled source names correspond to the objects considered in this work. Filled circles correspond to two flux states, quiescent and flaring, of the known TeV sources (figure courtesy of L. Costamante).

TABLE 1

PREDICTED TeV FLUX VALUES FOR THE BL LAC OBJECTS CONSIDERED IN THIS WORK

SOURCE	PREDICTED FLUX								OBSERVING TIME		
	$F(>0.3$ TeV)				$F(>1$ TeV)						
	FOSS (f.u.)	SSC (f.u.)	FOSS[a] (c.u.)	SSC[a] (c.u.)	FOSS (f.u.)	SSC (f.u.)	FOSS (c.u.)	SSC (c.u.)	Required (FOSS) (hr)	Required (SSC) (hr)	Exposure (hr)
1ES 0033+595.....	2.04	0.25	0.166	0.021	0.48	0.04	0.229	0.019	23	1482	12.02
1ES 0120+340.....	0.28	0.30	0.024	0.025	0.06	...	0.029	...	1135	1047	5.05
RGB J0214+517.....	5.93	0.07	0.483	0.006	1.43	6.2E−3	0.681	0.003	2.8	18107	6.05
1ES 0229+200.....	0.96	0.31	0.078	0.026	0.21	4.0E−3	0.100	0.002	101	968	14.69
1ES 0806+524.....	1.36	...	0.111	...	0.27	...	0.129	...	50	...	18.70
RGB J1117+202.....	1.17	0.10	0.095	0.008	0.28	...	0.133	...	68	10189	3.26
1ES 1553+113.....	0.20	0.42	0.016	0.035	0.02	...	0.010	...	2260	535	2.82
RGB J1725+118.....	12.80	0.015	1.043	0.001	3.52	1.0E−3	1.676	...	0.67	651240	2.33

NOTES.—Flux values are given in both absolute flux (f.u.: 10^{-11} ergs cm^{-2} s^{-1}) and Crab units (c.u.). Two estimates are given for each source, one obtained from the parameterization of the SED adapted from Fossati et al. 1998 (FOSS), the other from the SSC model by Costamante & Ghisellini 2002. Conversion to Crab units used a Crab flux above 0.3 TeV of $F_{\rm Crab}(>0.3\ {\rm TeV}) = 12.27 \times 10^{-11}$ ergs cm^{-2} s^{-1}. The observing time corresponds to the time needed for a 5 σ detection, given a sensitivity of $5.74/[t(h)]^{1/2}$ (Table 2). The actual time spent on source is also given as a reference.

[a] Flux values used to estimate the required observing time.

2. SELECTION OF AGNs FOR WHIPPLE OBSERVATIONS

We have chosen from the BL Lac object candidate list developed by Costamante & Ghisellini (2002) the most suitable candidates for TeV observations. We preferentially selected objects that culminate at an angle to the zenith $\Theta < 30^\circ$ and objects with redshifts smaller than 0.2, where opacity due to pair production is not so extreme as to prevent detection. Based on the prediction of Fossati et al. (1998), we required that the flux above 0.3 TeV should be greater than $\sim$10% of the Crab Nebula flux, so as to keep observing time below a reasonable value of $\sim$50 hr per source. In some cases the selection of objects was biased by the past record of X-ray activity, i.e., episodes of flaring activity.

After the selection criteria were applied, six objects were identified as the best target candidates for TeV observations by the Whipple 10 m telescope during the 2001–2002 observing season (circled sources in Fig. 1): 1ES 0033+595, RGB J0214+517, 1ES 0229+200, 1ES 0806+524, RGB J1117+202, and RGB J1725+118. However, at a higher redshift two extra objects, 1ES 0120+340 and 1ES 1553+113, were included in this work, since both belong to the list of TeV candidates and were observed in the same season by the Whipple telescope. The selection of these two objects was based on their extreme nature (Ghisellini 1999), both having many similarities in their broadband properties to 1ES 1426+428. Table 1 lists the selected objects, along with the predicted flux values.

3. OBSERVATIONS

Very high energy (VHE) observations reported here have been made with the Whipple Observatory 10 m gamma-ray telescope (Cawley et al. 1990) on Mount Hopkins in Arizona. Cerenkov radiation produced by gamma-ray– and cosmic-ray–induced atmospheric showers is recorded by a high-resolution camera located on the focal plane. The camera (Finley et al. 2001) is equipped with 379 0.°12 photomultiplier tubes (PMTs), giving a total field of view (FOV) of 2.°6 diameter. This inner part of the camera is surrounded by three circular rings of 111 0.°25 PMTs, which extend the FOV to 4° diameter. The telescope uses a hardware pattern-recognition trigger that suppresses accidental triggers due to the night sky background light (Bradbury 1999). Only the inner 331 PMTs participate in the telescope trigger. Although the signals from the outer 111 PMTs are recorded by the electronics, they are not involved in the analysis process used here. Table 2 shows the telescope's performance based on Crab Nebula observations, the standard candle for TeV astronomy, which were taken over the same period of time as the observations reported here. The telescope energy threshold (defined as the energy at which the response to a Crab-like source peaks) was $390 \pm 80_{\rm sys}$ GeV[17] during the same period of time.

Observations were carried out between 2001 October and 2002 July, with total observing times on individual sources ranging from a few hours to about 20 hr and restricted to

[17] For simplicity, $\pm 80_{\rm sys}$ is omitted hereafter.

TABLE 2

2000–2001 AND 2001–2002 WHIPPLE TELESCOPE SENSITIVITY, OBTAINED FROM CRAB NEBULA OBSERVATIONS

Observing Season	$\langle\Theta\rangle$[a] (deg)	Exposure (hr)	Excess Events (γ minute^{-1})	Background Events (counts minute^{-1})	Sensitivity ($\sigma/h^{1/2}$)
2000–2001.....	19.7	8.3	3.36 ± 0.20	8.66 ± 0.13	5.74
2001–2002.....	18.7	23.7	2.75 ± 0.10	5.88 ± 0.06	5.57

[a] Mean zenith angle of the observations.

TABLE 3

SUMMARY OF OBSERVATIONS OF 10 X-RAY–SELECTED BLAZARS DURING THE 2000–2001 AND 2001–2002 OBSERVING SEASONS WITH THE WHIPPLE 10 m TELESCOPE

	EQUATORIAL COORDINATES			OBSERVING PERIOD		WHIPPLE OBSERVATORY	
SOURCE	R.A. (J2000.0)	Decl. (J2000.0)	REDSHIFT	Season	MJD	Max. Ele. (deg)	$\langle\Theta\rangle$[a] (deg)
1ES 0033+595	00 35 52.63	+59 50 04.60	0.086[b]	2001 Oct–2002 Jan	52,193–52,283	62.1	29.0
1ES 0120+340	01 23 08.55	+34 20 47.50	0.272	2001 Oct–Nov	52,195–52,234	87.6	8.0
RGB J0214+517	02 14 17.93	+51 44 51.96	0.049	2001 Oct–2002 Jan	52,197–52,288	70.2	22.4
1ES 0229+200	02 32 48.46	+20 17 16.20	0.139	2001 Oct–2002 Jan	52,193–52,289	78.3	17.0
1ES 0806+524	08 09 49.15	+52 18 58.70	0.138	2001 Nov–2002 Mar	52,228–52,348	69.6	23.5
RGB J1117+202	11 17 06.20	+20 14 07.00	0.139	2001 Dec–2002 Feb	52,265–52,317	78.3	18.3
1ES 1426+428	14 28 32.66	+42 40 20.60	0.129	2001 Feb–Jun	51,940–52,073	79.3	19.0
1ES 1553+113	15 55 43.04	+11 11 24.38	0.360	2002 Apr–May	52,373–52,407	69.2	23.0
RGB J1725+118	17 25 04.36	+11 52 15.20	0.018	2002 Apr–Jul	52,374–52,460	69.9	22.0
1ES 1959+650	19 59 59.85	+65 08 54.67	0.048	2002 May–Jul	52,410–52,463	56.8	40.1

NOTES.—An observing season spans from September to July. Because of extreme weather conditions in southern Arizona, no observations are taken during August. Units of right ascension are hours, minutes, and seconds, and units of declination are degrees, arcminutes, and arcseconds. "Max. Ele." is the maximum elevation that the object reaches as observed from the Whipple observatory (latitude = N31°57′.6).

[a] Mean zenith angle of the observations.

[b] Tentative redshift.

zenith angles less than 30°. For comparison purposes, we also summarize observations on the detection at TeV energies of 1ES 1426+428 and 1ES 1959+650. The observations of 1ES 1426+428 reported in Horan et al. (2002) correspond to the period of time between 2001 February and June, when the object was observed most extensively, and a detection was claimed above a 5 σ level by the Whipple collaboration. 1ES 1959+650 data (Holder et al. 2003) are taken from observations of the source during a flaring state between 2002 May and July. All observations are summarized in Table 3.

The database consists of on-source observations, typically each of 28 minutes duration. A subset of observations are accompanied by control off-source observations, which target a region of the sky free from known gamma-ray sources. The off-source observation is taken directly before or after the on-source observation on a region offset 30^{m} in right ascension from the on-source region, thereby following the same elevation-azimuth path in the sky as the candidate source.

Predicted flux levels based on the parameterized SED of Fossati et al. (1998) (L. Costamante 2001, private communication) have been used to estimate how much on-source observing time would be required to achieve a 5 σ detection for each source. These flux estimates give us the most optimistic time exposure required to achieve a significant detection. Table 1 shows the predicted flux values, along with the required on-source observing time. Required observing times have been obtained based on the telescope sensitivity to a Crab-like source (and assuming background rates similar to those of the Crab off-source region).

The stability of cosmic-ray trigger rates and throughput factor, a measurement of the change in telescope efficiency according to the procedure described in LeBohec & Holder (2003), are monitored every observing night and have been used in this work to select individual data runs, in order to provide good-quality data sets.

4. ANALYSIS TECHNIQUE

The data have been subjected to the standard image processing analysis, in which recorded Cerenkov images are parameterized using a moment analysis (Hillas 1985). A set of image parameter cuts (Supercuts 2000), optimized on Crab Nebula data, was applied in order to identify candidate gamma-ray events based on the image shape (*width* and *length*), location (*distance*), and orientation (*alpha*; Reynolds et al. 1993). The image parameter domain used in this work in order to select gamma-ray candidate events is summarized in Table 4.

TABLE 4

IMAGE PARAMETER CUTS USED IN THIS WORK (SUPERCUTS 2000)

Parameter	Cut
Cleaning[a]	
Picture[b]	4.25 σ
Boundary	2.25 σ
Image	
Length	0°.13–0°.25
Width	0°.05–0°.12
Distance	0°.4–1°.0
Alpha	$\leq 15°$
Length/Size[c]	$<0°.0004$/d.c.[d]
Max1[e]	>30 d.c.[d]
Max2[e]	>30 d.c.[d]

[a] Only pixels with a significant signal above the background are considered as part of the image and thus used in the image parameterization. The signals in the rest of the pixels are set to zero and ignored in the analysis. This process is known as image cleaning. See Reynolds et al. 1993 for details.

[b] Three neighboring pixels have to be above the picture cut.

[c] Size refers to the sum of the intensities over the pixels that constitute the image, in d.c.

[d] d.c. = digital counts.

[e] Max1 and Max2 refer to the highest and second-highest pixel intensity in the image in d.c.

TABLE 5

SUMMARY AND RESULTS OF OBSERVATIONS OF THE X-RAY–SELECTED BL LAC OBJECTS CONSIDERED IN THIS WORK

Source	Mode	Exp. (hr)	$\langle\Theta\rangle$[a] (deg)	Raw Events	Events[b] (*alpha* $\leq 15^\circ$)	S (σ)	Rate[c] (γ minute^{-1})	$UL_{>0.39\,TeV}^{97\%\,c.l.}$ (c.u.)	$UL_{>0.39\,TeV}^{97\%\,c.l.}$ (f.u.)	$UL_{>1\,TeV}^{97\%\,c.l.}$ (c.u.)	$UL_{>1\,TeV}^{97\%\,c.l.}$ (f.u.)
1ES 0033+595.....	On	12.02	29	967,755	3794	0.42	0.05 ± 0.12	0.11	0.97	0.03	0.24
	Off	12.04	26	997,066	4023 (0.93)	...	(5.56 ± 0.09)	...	...	...	...
1ES 0120+340.....	On	5.05	8.0	436,321	1241	−0.49	-0.08 ± 0.16	0.12	1.00	0.03	0.25
	Off	7.44	10.1	647,953	2034 (0.62)	...	(4.55 ± 0.10)	...	...	...	...
RGB J0214+517.....	On	6.05	22.4	557,988	1923	0.64	0.11 ± 0.17	0.17	1.51	0.04	0.37
	Off	6.05	22.3	556,078	1860 (1.01)	...	(5.12 ± 0.12)	...	...	...	...
1ES 0229+200.....	On	14.69	17.0	1,341,365	4570	0.74	0.08 ± 0.11	0.11	0.97	0.03	0.24
	Off	15.82	15.0	1,439,227	4727 (0.95)	...	(4.98 ± 0.07)	...	...	...	...
1ES 0806+524.....	On	18.70	23.5	1,856,253	4956	0.14	0.01 ± 0.09	0.08	0.67	0.02	0.16
	Off	18.83	23.0	1,867,487	4942 (1.00)	...	(4.37 ± 0.06)	...	...	...	...
RGB J1117+202.....	On	3.26	18.3	348,436	933	0.47	0.10 ± 0.22	0.21	1.84	0.05	0.45
	Off	3.26	19.0	350,701	915 (0.99)	...	(4.69 ± 0.15)	...	...	...	...
1ES 1553+113.....	On	2.82	23.0	238,032	554	0.77	0.15 ± 0.20	0.19	1.62	0.05	0.40
	Off	3.72	22.3	326,616	743 (0.71)	...	(3.32 ± 0.12)	...	...	...	...
RGB J1725+118.....	On	2.33	22.2	187,298	489	0.67	0.15 ± 0.22	0.23	1.98	0.06	0.49
	Off	2.33	22.2	189,671	467 (1.00)	...	(3.34 ± 0.16)	...	...	...	...

NOTES.—Data have been analyzed using Supercuts 2000 (Table 4). Flux upper limits (UL) are given in units of f.u. $= 10^{-11}$ ergs cm^{-2} s^{-1}.

[a] Mean zenith angle of the observations.

[b] Events after image cuts (Supercuts 2000). The number in parentheses is the scaling factor (SCF).

[c] The number in parentheses is the background rate in counts minute^{-1}.

The aim of any analysis method is to estimate the mean number of photons coming from the source direction, which requires a reliable estimate of the number of background cosmic-ray events. Ideally, an equal exposure of on-source observations and control off-source observations is used; however, in an attempt to increase the total on-source exposure times, many runs are taken with no accompanying control off-source observations. Prior to this work, the background for these observations was directly estimated from the on-source observations themselves, using events with orientations (*alpha*) such that they are not from the direction of the source (Catanese et al. 1998). To avoid possible systematic effects introduced by this method when estimating the statistical significance of an excess, an alternative method of determining the number of background events has been considered. The concern is that in order to reach the predicted flux levels for the sources considered in this work, long exposure times are required to achieve a significant detection. We therefore need to ensure that systematic errors are kept to a minimum.

The method involves selecting *any* off-source observation recorded at similar elevations and preferably on the same night as the on-source observation of interest. This "matching" procedure is carried out qualitatively by comparing five different factors: date, throughput factor, mean elevation, mean sky noise, and number of pixels turned off during data taking (to avoid bright stars in the field of view). The first two are chosen to ensure that the telescope performance and weather conditions are the same for on-source and off-source observations. The other three parameters are chosen to ensure as much as possible that the shape of the image parameter distributions is similar within statistical fluctuations.

Once on/off matched pairs are obtained, standard on/off analysis is performed, including software padding (Cawley et al. 1993) to compensate for differences in sky brightness between the on-source observations and the corresponding control off-source observations. After matching and padding, the distribution of the parameter *alpha* for the on-source and off-source observations is obtained. Despite the care taken to match on-source and off-source observations, a remaining difference in the total number of events after image cuts, due largely to small differences in the zenith angles of the matched pairs, has still to be corrected for. This is done by introducing a scaling factor (SCF), which scales both *alpha* distributions, corresponding to the on-source and off-source observations, using the total number of events in the *alpha* region from 30° to 90°. Table 5 shows the SCF for the sources considered in this work (in parentheses in the column headed "Events"). Where genuine on/off pairs are available, these are added to the matched pairs before the *alpha* distributions are scaled.

When no significant excess of a signal over the background is found, it is possible to set an upper limit to the mean gamma-ray flux expected from the source direction. Calculations of flux upper limits depend on the number of background events and the number of events coming from the source direction. In this work, flux upper limits are calculated in several steps, in a similar way to the approach of Aharonian et al. (2000). First, the method of Helene (1983) is applied, to set an upper limit to the mean number of gamma-ray events expected from the source direction. When applying this method, we required that the number of background events always be smaller than the number of events coming from the source direction, i.e., that the mean number of source counts always be positive. If the opposite is true, a conservative approach is taken, and the number of events coming from the source direction is made equal to the number of background events. Second, the upper limit in source counts is converted into a fraction of the Crab Nebula flux by comparison with contemporaneous Crab Nebula observations (UL_C). The conversion into absolute flux units is straightforward using the Crab Nebula flux (Hillas et al. 1998) above the energy threshold, E_{th}, of the observations [$F_C(>0.39\ \mathrm{TeV}) = 8.30 \times 10^{-11}$ ergs cm^{-2} s^{-1}). A more general equation can be used (see eq. [1]) to obtain the upper limit using the Crab Nebula flux above any

given energy, E:

$$\mathrm{UL}(>E_{\mathrm{th}}) = \mathrm{UL}_{\mathrm{C}} F_{\mathrm{C}}(>E)\left(\frac{E_{\mathrm{th}}}{E}\right)^{-\alpha+1} \text{ ergs cm}^{-2}\text{ s}^{-1}\ . \quad (1)$$

This method assumes that the Crab Nebula flux is stable over time (Hillas et al. 1998) and that the differential spectrum (α) of the putative source is similar to that of the Crab Nebula ($\propto E^{-\alpha}$, where $\alpha = 2.49$). The only uncertainty to be taken into consideration on the flux upper limits is that introduced by the normalization of the Crab Nebula flux, i.e., the uncertainty in the Crab Nebula photon flux. Above the telescope energy threshold (390 GeV) the uncertainty is 25%, and above 1 TeV it is 10% (Catanese et al. 1998). The amount of IR absorption plays an important role in modeling the blazar SED at high energies (the emission models should account for the intrinsic spectra and not the IR absorbed ones), so estimates have been obtained for the amount of IR absorption expected in each case, according to the source redshift and assuming again a Crab-like source spectrum.

5. RESULTS

5.1. *Flux Upper Limits*

Table 5 summarizes the results of the complete set of observations of the eight selected sources. As this class of source is known to be highly variable, light curves (source count rates vs. time) have been used to search for episodes of emission on three different timescales: 28 minute, daily, and monthly. No evidence for variable VHE emission has been seen over any of these timescales. Flux upper limits are given at a 97% ($\sim 2\ \sigma$) confidence level (c.l.) in Crab and absolute flux units above the energy threshold of 390 GeV. Upper limits are also reported above 1 TeV by reducing the flux at 390 GeV by 75%, which assumes again a Crab-like spectrum.

Table 6 shows the flux upper limits derived in this work, as compared to the two predicted fluxes given in Costamante & Ghisellini (2002). The estimated percentage of absorption of the gamma-ray photon flux due to the IR background is also given. For two of the objects in our sample, RGB J0214+517 and RGB J1725+118, the flux upper limit, IR absorption–corrected, is below the value predicted by the adapted version of the Fossati parameterization above 0.3 TeV. According to this parameterization, the predicted fluxes are derived from SEDs that represent the average state of a source in a given radio luminosity range. The SEDs were derived including also those of the known TeV blazars; therefore, it is considered that the derived flux estimates from these SEDs are more representative of a high emission state. On the contrary, the SSC model considered (Ghisellini et al. 2002) is designed to fit only the synchrotron spectra of the sources, more representative of a quiescent state. The IC component is then inferred from the synchrotron one. Upper limits derived in this work do not contradict the SSC-predicted TeV emission above 0.3 TeV, since in all cases our flux upper limits are well above the predicted value. For 1ES 0229+200, there is a flux prediction above 0.3 TeV of 0.02 Crab units (c.u.) by Stecker et al. (1996). Our flux upper limit on this source is not in contradiction with this.

The flux upper limits derived in this work have been compared with those previously available from the CAT (Piron 2000) and HEGRA (Tluczykont et al. 2003) experiments, where available (Table 6). A direct comparison of flux upper limits derived by the different experiments shows that they are of the same order of magnitude. For the sources listed in Table 6, flux upper limits derived by different experiments

TABLE 6

Comparison between Predicted and Measured TeV Fluxes for the BL Lac Objects Considered in This Work

	Flux Prediction [$F(>0.3$ TeV)]				Whipple $\mathrm{UL}^{97\%\,\mathrm{c.l.}}$			CAT[e]	HEGRA[f]
Source	FOSS[a] (c.u.)	SSC[a] (c.u.)	Stecker[b] (c.u.)	IR[c] (%)	Above 390 GeV (c.u.)	Above 300 GeV[d] (c.u.)	Above 300 GeV, IR-corrected (c.u.)	[$F(>0.25$ TeV)] $\mathrm{UL}^{99.7\%\,\mathrm{c.l.}}$ (c.u.)	$\mathrm{UL}^{99.9\%\,\mathrm{c.l.}}$ (c.u.)
1ES 0033+595.....	0.17	0.021	...	46	0.11	0.16	0.23	0.45	...
1ES 0120+340.....	0.02	0.025	...	88	0.12	0.18	0.34	...	$0.04_{>0.75\,\mathrm{TeV}}$
RGB J0214+517.....	0.48	0.006	...	30	0.17	0.25	0.32	0.39	...
1ES 0229+200.....	0.08	0.026	0.02	63	0.11	0.16	0.26	...	$0.17_{>0.78\,\mathrm{TeV}}$
1ES 0806+524.....	0.11	...	...	63	0.08	0.12	0.19	0.67	$0.29_{>0.86\,\mathrm{TeV}}$
RGB J1117+202.....	0.09	0.008	...	63	0.21	0.31	0.50	...	...
1ES 1553+113.....	0.02	0.035	...	95	0.19	0.28	0.55	...	...
RGB J1725+118.....	1.04	0.001	...	12	0.23	0.34	0.38	...	$0.08_{>0.76\,\mathrm{TeV}}$

Notes.—Whipple values correspond to the ones obtained in this work. Predicted flux values have been converted into Crab units using the integral Crab flux, $F_{\mathrm{C}}(>0.3\ \mathrm{TeV}) = 12.27 \times 10^{-11}$ ergs cm^{-2} s^{-1}. The predicted fluxes are given by the modified version of the parameterization of the SED according to Fossati et al. 1998 and the SSC model, both described in Costamante & Ghisellini 2002. Predicted flux values are also given according to Stecker, de Jager, & Salomon 1996 where available.

[a] Costamante & Ghisellini 2002.

[b] Stecker et al. 1996.

[c] Using the optical depth given in de Jager & Stecker 2002. Estimated absorption of the gamma-ray photon flux between 300 GeV and 10 TeV, assuming a Crab-like spectrum.

[d] The correction has been done by assuming a Crab-like integral spectrum. Upper limits are increased by 48% when going from 390 to 300 GeV.

[e] Piron 2000.

[f] Tluczykont et al. 2003.

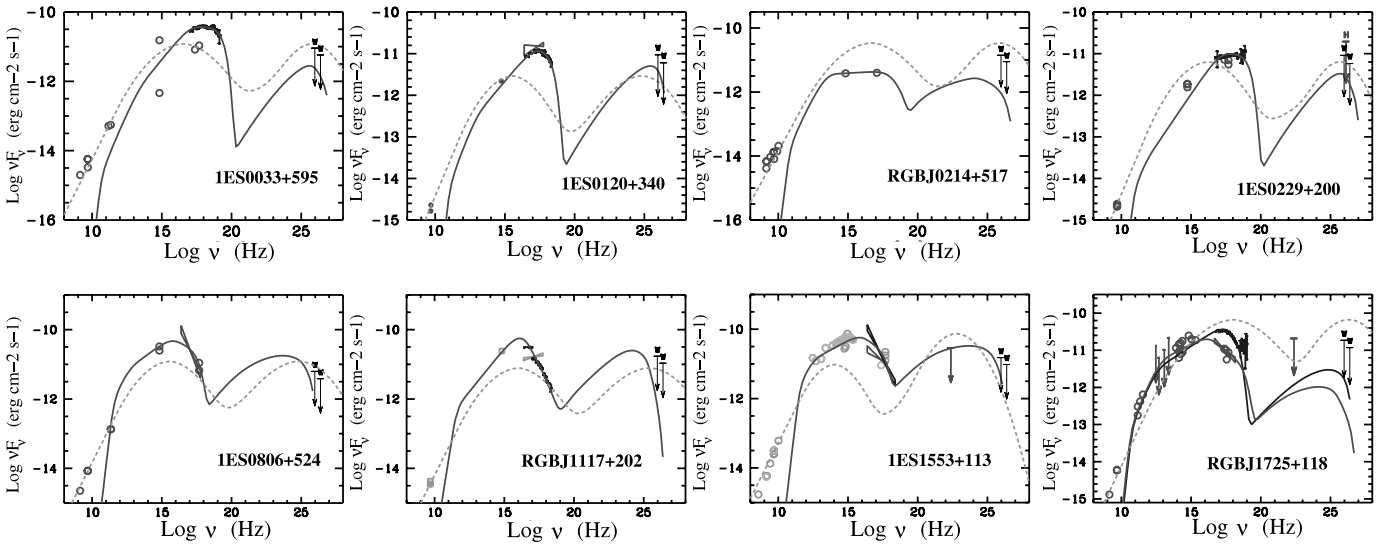

FIG. 2.—SSC model (*solid line*) and phenomenological parameterization of Fossati et al. (1998), as modified by Costamante & Ghisellini (2002) (*dashed line*): from top left to bottom right, 1ES 0033+595, 1ES 0120+340, RGB J0214+517, 1ES 0229+200, 1ES 0806+524, RGB J1117+202, 1ES 1553+113, and RGB J1725+118. Flux upper limits obtained in this work are represented by arrows labeled "W" at two energies, 390 GeV and 1 TeV. The HEGRA flux upper limit for 1ES 0229+200 has been labeled "H" (figure courtesy of L. Costamante).

cannot be used to invalidate each other, since observations are not contemporaneous.

Figure 2 shows the SED of the eight objects as described by an SSC model (*solid lines*) and by the adapted phenomenological parameterization of Fossati (*dashed lines*; Costamante & Ghisellini 2002). Flux upper limits obtained in this work are represented by arrows labeled "W" at two energies, 390 GeV and 1 TeV.

We note in addition that, because of the time variability of high-energy emission from these objects, the upper limits reported in this work are only valid for the period of time during which observations were carried out.

5.2. *ASM X-Ray Fluxes*

The X-ray flux of the sources in our sample can provide an indication of whether enhanced TeV emission was expected over the period of the gamma-ray observations. According to the SSC model, if the same population of electrons is responsible for the two peaks observed in the blazar SED, an increase in the synchrotron photon flux would lead to a corresponding increase in the IC photon flux. In BL Lac objects the behavior of the most energetic electrons is well monitored in the X-ray band (dominated by the synchrotron emission) and in the GeV–TeV band (dominated by IC emission). In fact, strong correlation has been observed between the fluxes in the X-ray and GeV–TeV bands, which matches the predictions of the IC models (e.g., observations of Mrk 501 in 1997 [Catanese et al. 1997b; Pian et al. 1998; Krawczynski et al. 2000] and of Mrk 421 in 1995 [Buckley et al. 1996] and 2001 [Holder et al. 2001]).

Data from the ASM on board *RXTE* were available for five of the eight sources in our sample, covering the period from 1997 January 1 to 2002 July 31. We calculated the mean X-ray flux over the exact period of time in which the TeV gamma-ray observations reported here were taken, the average over the years 1997–2002, and the average on a yearly basis (see Table 7). This mean flux over long periods of time is not very representative for these types of objects, which show very strong variability in their emission states over a range of timescales from hours to years; however, from the comparison of these mean fluxes we conclude that the mean X-ray flux over the period of time in which the TeV gamma-ray observations were taken does not increase significantly from the mean over all years for any of the sources. Only 1ES 0806+524 shows a marginally higher than average X-ray flux during the year 2002 (in which gamma-ray observations were taken), 2.7 σ above the average X-ray flux over all years.

As a comparison, we have proceeded in the same way using ASM data corresponding to the known TeV sources Mrk 421, Mrk 501, 1ES 1426+428, and 1ES 1959+650 and present the results in Table 7. In the cases of 1ES 1426+428 and 1ES 1959+650, the mean X-ray flux during the period of time in which the TeV detection observations were taken is significantly higher than the mean over all years. Mrk 421 and Mrk 501 show a higher-than-average X-ray flux over the years 2001 and 1997, respectively; it is, in fact, over those two years that both objects showed periods of the highest gamma-ray activity observed (flux levels of up to 13 times that of the Crab Nebula in the case of Mrk 421 [Krennrich et al. 2002] and up to 4 times that of the Crab Nebula in the case of Mrk 501 [Catanese et al. 1997b]). However, there have been occasions when rapid X-ray or TeV flares have been seen without a corresponding flux variation in the other energy band (e.g., Mrk 501 [Catanese & Sambruna 2000] and 1ES 1959+650 [Krawczynski 2004]).

From this simple study it is inferred, if we assume that the properties described above are representative of the general behavior of BL Lac objects, that it is possible to use the mean X-ray flux, at least over long timescales, as an indicator of source activity, which in turn could result in enhanced emission of TeV gamma rays. Our sources show no evidence of a long-lasting period of high activity, as indicated by the average X-ray flux, over the period of time in which our TeV observations took place. Even for the well-established TeV sources Mrk 421 and Mrk 501, there are periods of time

TABLE 7
MEAN *RXTE* (ASM) X-RAY FLUXES DURING VARIOUS TIME PERIODS FOR THE SOURCES IN THIS WORK

Name	1997–2002[a] (mcrab)	1997 (mcrab)	1998 (mcrab)	1999 (mcrab)	2000 (mcrab)	2001 (mcrab)	2002[a] (mcrab)	γ_{Obs}[b] (mcrab)
1ES 0120+340.....	2.15 ± 0.11	...	2.52 ± 0.27	2.74 ± 0.22	1.25 ± 0.23	2.35 ± 0.25	1.63 ± 0.36	2.33 ± 0.71
RGB J0214+517.....	1.66 ± 0.08	1.72 ± 0.14	1.54 ± 0.17	1.61 ± 0.21	1.78 ± 0.20	1.70 ± 0.22	1.49 ± 0.27	0.89 ± 0.37
1ES 0229+200.....	1.78 ± 0.08	2.64 ± 0.16	1.20 ± 0.17	1.11 ± 0.22	1.70 ± 0.20	1.86 ± 0.24	2.10 ± 0.31	1.05 ± 0.37
1ES 0806+524.....	1.51 ± 0.07	1.07 ± 0.15	1.57 ± 0.15	1.42 ± 0.18	1.48 ± 0.18	1.85 ± 0.19	2.19 ± 0.24	1.84 ± 0.29
Mrk 421	8.68 ± 0.07	6.20 ± 0.16	12.52 ± 0.19	4.83 ± 0.19	12.60 ± 0.19	14.03 ± 0.23	7.69 ± 0.24	19.88 ± 0.29[c]
1ES 1426+428.....	2.88 ± 0.08	2.30 ± 0.18	2.99 ± 0.17	2.68 ± 0.19	3.22 ± 0.19	3.42 ± 0.20	2.75 ± 0.22	3.69 ± 0.33
Mrk 501	7.32 ± 0.06	15.57 ± 0.16	7.65 ± 0.15	5.69 ± 0.16	5.39 ± 0.17	4.26 ± 0.17	4.34 ± 0.21	17.35 ± 0.27[d]
RGB J1725+118.....	2.64 ± 0.09	2.65 ± 0.20	2.40 ± 0.20	2.54 ± 0.22	1.98 ± 0.23	3.16 ± 0.22	3.27 ± 0.30	2.56 ± 0.44
1ES 1959+650.....	3.75 ± 0.06	2.57 ± 0.12	2.62 ± 0.14	4.06 ± 0.14	5.05 ± 0.16	4.54 ± 0.15	4.77 ± 0.19	6.48 ± 0.39

NOTE.—The mean flux in each case is the weighted mean for the appropriate interval.
[a] Extends only up to 2002 July.
[b] Refers to the period of time in which TeV observations were taken.
[c] Period from 2000 November to 2001 May.
[d] Period from 1997 March to June.

in which the TeV fluxes fall below the sensitivity of current Cerenkov telescopes and are not detected, corresponding to periods of low X-ray activity (e.g., Piron et al. 2001). Also, it is inferred that the level of the mean X-ray flux can be used as a potential indicator of gamma-ray activity and might trigger follow-up gamma-ray observations.

6. DISCUSSION

In this work we have observed a set of BL Lac objects selected from a sample of promising candidates for TeV emission developed by Costamante & Ghisellini (2002). This sample is comprised of objects that show high radio and X-ray fluxes, since in order to produce a strong TeV signal by the IC process, a large number of energetic electrons and seed photons are required. These authors have also provided estimates of the TeV fluxes according to a detailed SSC emission model, which can be used both to establish the detectability of this sample of objects and to test the model itself. Our TeV observations have resulted in a set of flux upper limits, above an energy of 390 GeV, that do not conflict with the predicted values according to current SSC models. We investigate here the possible reasons for these nondetections.

The first possibility is that the TeV fluxes are far below the sensitivity of current Cerenkov telescopes. The SSC model used to derive the flux estimates at TeV energies predicts TeV fluxes more representative of a quiescent state of the sources, and the estimated times required to guarantee a 5 σ detection are all above 500 hr (see Table 1). Considering that the available observing time with the Whipple telescope amounts to 700–800 hr per season, spending 500 hr of an observing season on a single source is not feasible. The current sensitivity of the Whipple telescope does not allow us to test the detectability of this sample of objects; i.e., our TeV observations do not allow a test of this SSC model. However, the next generation of Cerenkov telescopes, such as VERITAS-4 (Weekes et al. 2002), with a sensitivity above 300 GeV of 8×10^{-13} ergs cm^{-2} s^{-1} (5 mcrab) on a Crab-like source spectrum (50 hr for a 5 σ detection), would be able to reach the predicted flux levels in just a few hours of observations.

The second reason for our nondetections lies in the fact that the sources were not in a high flux emission state. Our simple study in § 5.2 suggests that, at least for long-lasting flares, there is a correlation between X-ray and gamma-ray fluxes for the well-established TeV blazars. We have shown that, for some of the objects in our sample, the ASM X-ray fluxes show no significant increase over the period of time during which the TeV observations reported here took place. Therefore, we may not have detected these objects at TeV energies because they were in a low flux emission state during this period of time.

Another possible reason for our nondetections could be that the sample used to select targets for TeV observations does not provide a reliable list of candidate BL Lac objects for TeV emission. However, this explanation is weakened by the recent detections of 1ES 1426+428 and 1ES 1959+650 at TeV energies. These two objects belong to the candidate list developed by Costamante & Ghisellini (2002) and have been detected at different emission states. The detection of 1ES 1426+650 by the Whipple collaboration came as a result of a long observing campaign during the year 2001, and since then there has been no strong evidence for TeV emission. On the contrary, 1ES 1959+650 was detected on a nightly basis in a flaring state at a flux level of up to 5 c.u. in 2002 May–July. Since then no significant detection has been reported for that source. Because of the extreme variability that this type of object exhibits, our nondetections should not discourage future observations of objects selected from this sample.

The detection of 1ES 1959+650 at TeV energies could be seen as an example to encourage future observations of this sample of objects. A flux upper limit of $F^{99.9\%\,\mathrm{c.l.}}_{E>0.35\,\mathrm{TeV}} = 0.13$ c.u. was derived by Catanese et al. (1997a) from observations in 1996, far above the flux level of 3 mcrab, above 0.3 TeV, predicted by the SSC model. With the Whipple telescope sensitivity, at a flux level of 3 mcrab more than 26,000 hr of observations would have been required to achieve the detection of a gamma-ray signal at a 5 σ level. However, the HEGRA collaboration reported the detection of this source in a more quiescent state from ~95 hr observations during 2000 and 2001 with the HEGRA system of telescopes (Aharonian et al. 2003). The VHE flux reported for this source during that period of time was at a level of 5.3% that of the Crab Nebula. At this level, 250 hr of observations with the Whipple telescope would be required for a significant detection.

Further work is in progress to extend the list of objects bright in both the X-ray and the radio bands without preselection for source type. The *ROSAT* Bright Source Catalogue (Voges et al. 1999) has been used to produce a list of objects that would fall in the region delimited by Figure 1. 3C 120 ($z = 0.0334$) was selected from this list as one of the brightest objects in both bands. 3C 120 is a Seyfert I galaxy, with the angle between the jet and the line of sight less than 20°. Whipple observations (7.5 hr) during the 2002–2003 observing season resulted in a flux upper limit of 1.74×10^{-11} ergs cm^{-2} s^{-1} (20% that of the Crab Nebula). Also, very recently, a work by Padovani et al. (2003) has identified a new population of flat-spectrum radio quasars (FSRQs) with SEDs resembling those of high-energy–peaked BL Lac objects, which are potential candidates for TeV emission. Observations of these new types of candidate, as well as continuing observations of the sources discussed in this paper, are in progress now with the Whipple telescope and will continue with the telescope array system VERITAS-4, which is currently under construction.

The VERITAS collaboration is supported by the US Department of Energy, the NSF, the Smithsonian Institution, PPARC (UK), and Enterprise Ireland. We acknowledge the technical assistance of E. Roache and J. Melnick. We thank L. Costamante for his help and comments, as well as J. Holder for assistance and discussions throughout this work.

REFERENCES

Aharonian, F. A., et al. 2000, A&A, 353, 847
———. 2003, A&A, 406, L9
Bloom, S. D., & Marscher, A. P. 1996, ApJ, 461, 657
Bradbury, S. M. 1999, Proc. 26th Int. Cosmic Ray Conf. (Salt Lake City), 5, 263
Buckley, J. H. 1999, Astropart. Phys., 11, 119
Buckley, J. H., et al. 1996, ApJ, 472, L9
Catanese, M., & Sambruna, R. M. 2000, ApJ, 534, L39
Catanese, M., et al. 1997a, ApJ, 487, L143
———. 1997b, Proc. 25th Int. Cosmic Ray Conf. (Durban), 3, 277
———. 1998, ApJ, 501, 616
Cawley, M. F., et al. 1990, Exp. Astron., 1, 173
———. 1993, in Towards a Major Atmospheric Cherenkov Detector II, ed. R. C. Lamb (Ames: R. C. Lamb), 176
Chadwick, P. M., et al. 1999, ApJ, 513, 161
Costamante, L., & Ghisellini, G. 2002, A&A, 384, 56
de Jager, O. C., & Stecker, F. W. 2002, ApJ, 566, 738
Dermer, C. D., & Schlickeiser, R. 1993, ApJ, 416, 458
Finley, J. P., et al. 2001, Proc. 27th Int. Cosmic Ray Conf. (Hamburg), 7, 2827
Fossati, G., Maraschi, L., Celotti, A., Comastri, G., & Ghisellini, G. 1998, MNRAS, 299, 433
Ghisellini, G. 1999, Astropart. Phys., 11, 11
Ghisellini, G., Celotti, A., & Costamante, L. 2002, A&A, 386, 833
Ghisellini, G., & Madau, P. 1996, MNRAS, 280, 67
Gould, R. J., & Schréder, G. P. 1966, Phys. Rev. Lett., 16, 252
Helene, O. 1983, Nucl. Instrum. Methods Phys. Res., 212, 319
Hillas, A. M. 1985, Proc. 19th Int. Cosmic Ray Conf. (La Jolla), 3, 445
Hillas, A. M., et al. 1998, ApJ, 503, 744
Holder, J., et al. 2001, Proc. 27th Int. Cosmic Ray Conf. (Hamburg), 7, 2613
———. 2003, ApJ, 583, L9
Horan, D., et al. 2002, ApJ, 571, 753
Krawczynski, H. 2004, ApJ, in press
Krawczynski, H., Coppi, P. S., Maccarone, T., & Aharonian, F. A. 2000, A&A, 353, 97
Krennrich, F., et al. 2002, ApJ, 575, L9
LeBohec, S., & Holder, J. 2003, Astropart. Phys., 19, 221
Nishiyama, T., et al. 1999, Proc. 26th Int. Cosmic Ray Conf. (Salt Lake City), 3, 370
Padovani, P., Perlman, E. S., Landt, H., Giommi, P., & Perri, M. 2003, ApJ, 588, 128
Pian, E., et al. 1998, ApJ, 492, L17
Piron, F. 2000, Ph.D. thesis, Univ. Paris-Sud
Piron, F., et al. 2001, A&A, 374, 895
Primack, J. R., Bullock, J. S., Somerville, R. S., & MacMinn, D. 1999, Astropart. Phys., 11, 93
Punch, M., et al. 1992, Nature, 358, 477
Quinn, J., et al. 1996, ApJ, 456, L83
Reynolds, P. T., et al. 1993, ApJ, 404, 206
Sikora, M. 1994, ApJS, 90, 923
Sikora, M., Begelman, M. C., & Rees, M. J. 1994, ApJ, 421, 153
Stecker, F. W., de Jager, O. C., & Salamon, M. H. 1996, ApJ, 473, L75
Tluczykont, M., et al. 2003, in Proc. 28th Int. Cosmic Ray Conf. (Tsukuba), in press
Urry, C. M., & Padovani, P. 1995, PASP, 107, 803
Voges, W., et al. 1999, A&A, 349, 389
Weekes, T. C., et al. 2002, Astropart. Phys., 17, 221